UDC 551.513.2:551.465.7

INTERTROPICAL CONVERGENCE ZONE STUDIED WITH AN INTERACTING ATMOSPHERE AND OCEAN MODEL [1]

ARTHUR C. PIKE

Rosenstiel School of Marine and Atmospheric Sciences, Division of Atmospheric Science, University of Miami, Coral Gables, Fla.

ABSTRACT

A simple, two-layer numerical model of the upper tropical ocean has been added to a pre-existing primitive-equation model of a zonally symmetric tropical atmosphere to predict a north-south profile of sea-surface temperature and its relationship to the atmospheric intertropical convergence zone (ITCZ). With an initially flat temperature profile near the Equator, it is found that a cold equatorial surface progressively develops as a result of upwelling and vertical mixing in the sea. A single ITCZ establishes itself at first over the Equator, but then migrates poleward as the Equator cools; the convergence zone remains single, despite the eventual double surface-temperature maximum. This marked hemispheric asymmetry is in accord with satellite observations.

1. INTRODUCTION

This paper is a continuation of a study by Pike (1968) involving numerical modeling of the atmospheric ITCZ (intertropical convergence zone) with the primitive equations. It was found in that study that, at least over the sea, the maximum upward motion and precipitation rate associated with the ITCZ occurred at or very near the latitude of maximum surface temperature. In particular, a notable equatorial surface-temperature minimun seemed to be essential if the ITCZ were to reach an equilibrium location away from the Equator. All these past numerical experiments were conducted with a 10 level two-dimensional atmospheric model with prescribed latitudinal surface-temperature profiles; some further results with this type of work will be discussed in section 2.

Clearly, though, the surface-temperature distribution, especially at sea, is not at all independent of atmospheric factors; the pattern of wind stress on the sea surface will strongly influence the upper ocean current system and its associated horizontal divergence. The resulting field of oceanic vertical motion, in conjunction with the well-known decrease of temperature with depth in the sea, can produce anomalously cold surface temperatures by means of upwelling. The development of relatively vigorous wind-driven ocean currents in themselves can, of course, induce substantial vertical turbulent mixing that would tend to lower the surface temperature. In a reverse sense, the direct thermodynamic effect of the surface-temperature pattern on the atmosphere is sure to affect its hydrostatic pressure gradient and the associated wind and wind-stress fields; there is a continuous two-way interaction between air and sea. Seemingly desirable, therefore, is to have the surface temperature a predicted rather than a fixed quantity in any model with a behavior strongly dependent on it. At sea, prediction of surface temperature requires approximation of the circulation of the upper ocean; in section 3, the structure of a simple, highly parameterized two-layer ocean model is described in detail. This device for surface-temperature prediction has been combined with the previously developed atmospheric model to make a fully interacting two-fluid numerical experiment over 88 days; the interesting results are presented in section 4. It then becomes possible in section 5 to compare the theoretical work with certain published satellite observations of cloud patterns in tropical latitudes.

2. RESULTS FROM A FORCED ATMOSPHERIC MODEL

As background material to the two-fluid experiment to be presented later, a brief description of the atmospheric part of the theoretical modeling will now be given, followed by two examples of its response to different fixed surface-temperature profiles. Its dynamics and thermodynamics are based on the model of Estoque and Bhumralkar (1969), with the addition of a moisture continuity equation and the inclusion of convective vertical mixing of moisture and latent heat as described by Estoque (1968). The air model, being zonally symmetric, is two-dimensional in latitude and height; it is based on marching forward in time the two horizontal momentum equations, the thermodynamic equation in terms of potential temperature and an equation of continuity for moisture. Pressures are hydrostatic; the field of vertical motion is computed from that of meridional motion using the steady-state approximation of the mass continuity equation. Both vertical and horizontal mechanical mixing of momentum, heat, and moisture are parameterized as in Estoque and Bhumralkar (loc. cit.); but the horizontal diffusivity has been increased to 10^{10} cm^2/s, the magnitude reported by Murgatroyd (1969) for synoptic scale motions. Vertical convective mixing of these properties is approximated by distributing their vertical fluxes with height in proportion to a buoyant parcel temperature excess, providing both the flux and the excess exist; sufficient care is taken not to

[1] Contribution No. 1353 from the University of Miami, Rosenstiel School of Marine and Atmospheric Sciences

duplicate the vertical advection process. A climatological radiational cooling, variable with height only, is used. Precipitation is computed as the sum of large-scale condensation, indicated by the moisture equation's prediction of supersaturation, and convective scale condensation, represented as a relative-humidity-dependent condensed fraction of the convective vertical moisture flux.

Spatially, the domain of numerical integrations runs from 34°S to 34°N and from the sea surface to the mean tropical tropopause at 16.5 km. The horizontal grid spacing is 2° of latitude except poleward of 26° latitude where it is 4°. There are 10 grid levels in the vertical, at 0, 9, 35, 590, 1545, 3171, 5870, 9647, 12,353, and 16,535 m above sea level. Important boundary conditions are: temporally constant values of all properties at the lateral boundaries, correction of the predicted horizontal divergence field to yield zero vertical motion at both the surface and the tropopause, and—for each of the two cases of this section—a constant imposed sea-surface temperature profile. The time step, forward except for the Coriolis terms which alone are backward-differenced to avoid weak instability, is restricted to one-eighth of an hour to avoid gravity-wave amplification. Advective space differencing is upstream to provide computational stability. Of course, this upstream differencing introduces an artificial kinetic-energy sink into the model. In our experiments, however, it is highly correlated with and about half the size of the pressure-gradient source; thus, it never threatens to run down the total kinetic energy, in general agreement with the results of Rosenthal (1970). All other space differencing, as for horizontal pressure gradients and the mass divergence, is centered.

The initial wind field is geostrophic, zonal, and nondivergent; initial temperatures, and therefore pressures, and relative humidities are annual Northern Hemisphere climatological means derived from MIT General Circulation Project data; see Peixoto (1960) and Peixoto and Crisi (1965).

The following two cases are identical, excepting their fixed surface-temperature profiles. Figure 1 shows the initial surface *potential* temperature profile for case I, in which this temperature is constant within 14° latitude of the Equator, but drops off at higher latitudes. The corresponding ordinary temperature profile, held constant in time, would show a small equatorial minimum about 0.3°C lower than at latitude 14°, as a result of the surface pressure having an equatorial minimum. Directly above the potential temperature profile is the 12-day accumulated precipitation profile for this case. There is a sharp peak of 35 cm directly on the Equator, indicating an active equatorial convergence zone. This rate of precipitation corresponds to about 1060 cm/yr, three times the observed amount in the heart of the actual ITCZ at atoll stations like Funafuti; see U.S. Weather Bureau (1959). However, the actual ITCZ is seldom observed right on the Equator, as will be shown in section 5 on satellite observations.

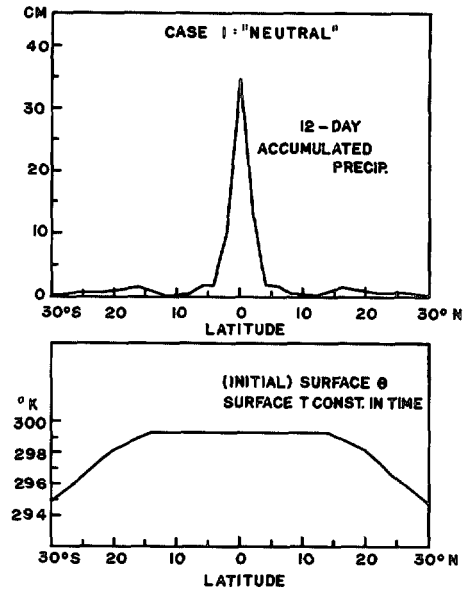

FIGURE 1.—Surface initial potential temperature and precipitation profiles, neutral case I.

Figure 2 shows the evolution of the 9.6-km vertical motion profile for case I; this altitude is very near the main level of nondivergence. At the initial time, of course, there is no vertical motion at all. One day later, as indicated by the solid line, a transient double updraft has developed at 6°S and 6°N. There is thereafter a progressive consolidation of this double feature; by 3 days, as indicated by the dotted line, a pronounced single updraft is right on the Equator. This single equatorial updraft appears to be very stable, as indicated by the vertical motion profile at 12 days, which is hardly different from that at 3 days. It is supposed that the initial transient double feature is induced by frictional convergence; the consolidation of it into a single updraft may well be aided by horizontal convergence of eddy heat flux from the two convection zones toward the Equator. Once the single updraft has been established, its apparently great stability against physical and numerical perturbations prevents a breakdown into the double mode; the other cases presented in this article exhibit the same characteristics.

Before going on to case II, it should be mentioned that the original work by Pike (1968) included an experiment carried out with a fixed surface-temperature profile showing a definite maximum on the Equator. The results were very similar to those for case I, with a very small equatorial minimum, indicating that the qualitative structure of the ITCZ is not affected by this kind of temperature-profile change.

In marked contrast to the above cases is case II where the surface-temperature profile has a fixed double maximum off the Equator at 8°S and 8°N and a *pronounced* minimum on the Equator. Figure 3 presents this new profile, similar in character to that which develops from

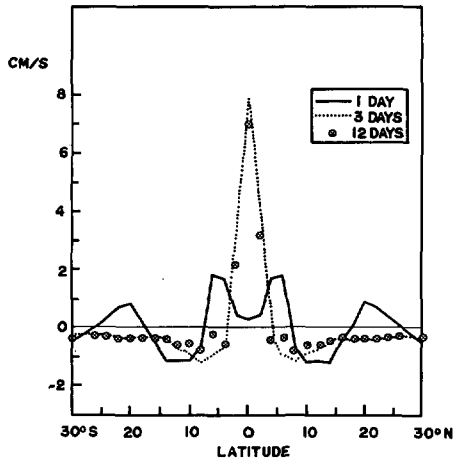

FIGURE 2.—Evolution of vertical motion at 9.6 km, case I.

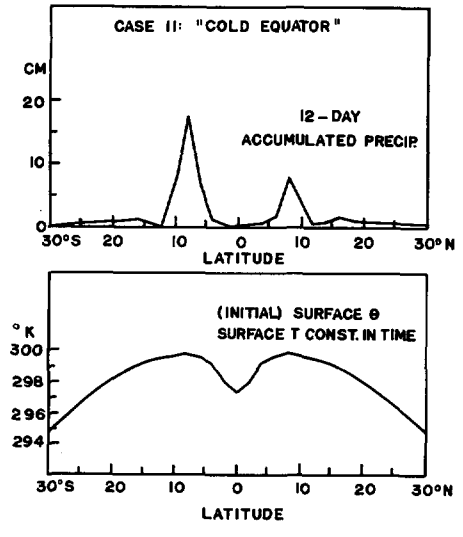

FIGURE 3.—Surface initial potential temperature and precipitation profiles, cold Equator case II.

cold equatorial upwelling and vertical mixing in the sea; see section 4 for an appropriate experimental example. Directly above the cold-Equator temperature profile is drawn the corresponding 12-day accumulated precipitation profile. A double maximum off the Equator, and directly over the latitudes of warmest surface water, is clearly indicated. Note that a marked hemispheric asymmetry in precipitation has developed, despite the symmetric thermal forcing and other boundary conditions; this asymmetry has plainly been generated internally, probably by truncation error in solving a second-order differential equation for height-averaged pressure by marching, with successive approximations, in latitude from 30°S to 30°N. Analytical details of this kind of pressure computation are given by Estoque and Bhumralkar (loc. cit., sec. 4); the finite-difference scheme for solving the second-order equation is described in Richtmyer and Morton (1967, sec. 8.5). The mean of the two maxima is about 12 cm,

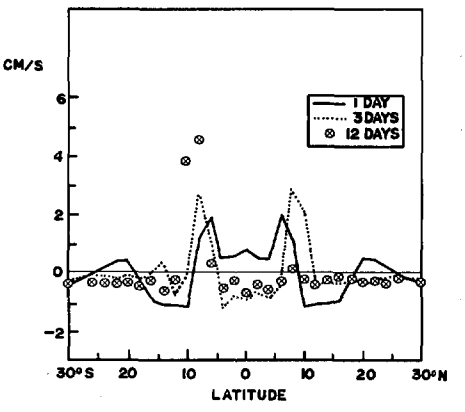

FIGURE 4.—Evolution of vertical motion at 9.6 km, case II.

corresponding to 365 cm/yr, very close to the actually observed oceanic ITCZ precipitation rate peak.

The vertical motion profiles of case II are shown in figure 4. At 1 day, indicated by the solid line, the 9.6-km profile is very similar to the corresponding one for case I. By 3 days, however, there is no indication of updraft consolidation; in fact, a modest equatorial downdraft is in evidence while the updrafts have moved to be over the warmest surface water. Influenced by the above truncation error, one updraft has become much stronger than the other at 12 days while the equatorial downdraft persists; in this model, the double ITCZ seems to be a metastable state analogous to a balanced seesaw that is easily tipped into a more stable position with one end, or branch, predominant. It is supposed that the lack of updraft consolidation in case II is a result of equatorial surface cooling, which can counteract the effect of horizontal eddy heat-flux convergence. That the dominant updraft formed in the Southern Hemisphere rather than more realistically in the Northern Hemisphere is a numerical accident; one cannot expect small numerical perturbations in a meridional plane model to have precisely the same effect as real asymmetric forcing in a three-dimensional atmosphere. The important point is that the model ITCZ prefers, as does the real atmosphere's, a single mode: see Hubert et al. (1969).

Of the two cases presented, the second (with a marked sea-surface temperature minimum on the Equator) appears to be the more realistic for the open ocean, far from insular or continental influence. The hemispherically symmetric surface-temperature profile for this case was taken from Defant (1961) and is an average of both the Northern Hemisphere and Southern Hemisphere data at longitude 135°W in the east-central Pacific.

In summary for the forced atmosphere model: experiments with it so far suggest that ITCZ structure is intimately related to the meridional surface temperature profile, at least over the sea. Given hemispherically symmetric conditions at the surface and in the subtropical atmosphere, a single equatorial convergence zone appears

to be the equilibrium state unless there is a marked surface-temperature minimum there, probably caused by oceanic upwelling and vertical mixing. Then, as is usually the case in the real atmosphere, the ITCZ will form several degrees of latitude away from the cold Equator; it may be double, with a branch in each hemisphere, or, as is more likely, it will become single if one of its branches reaches sufficient strength to suppress the other. As no definitive experiments with hemispherically asymmetric surface conditions, etc., have yet been made with this model, there are so far no conclusions regarding the seasonal variability of the actual ITCZ.

3. THEORETICAL BASIS OF THE SEA MODEL

Our simple ocean model for the prediction of sea-surface temperature approximates the real ocean by assuming an active surface mixed layer of variable depth h overlying an inert lower layer of infinite depth. As in the model of Kraus and Turner (1967), the real thermocline of finite thickness is replaced by an abrupt decrease in sea temperature from the mixed-layer value T to the lower underlayer value T_0 occurring at depth h. As in the air model, the predictive equations are primitive in form with only one horizontal dimension—that of latitude. They are 4 in number, predicting the *northward* x component of surface current u and the *westward* y component of surface current v, as well as T and h. The u and v equations are in momentum form, the T equation is a form of the first law of thermodynamics for an incompressible fluid, and the h equation is an equation of continuity. Explicitly, we have

$$\frac{\partial u}{\partial t}=-u\frac{\partial u}{\partial x}-\frac{E^*u}{h}+\frac{\tau_{0x}}{\rho h}-\frac{\partial}{\partial x}(g'h)+fv+\frac{1}{h}\frac{\partial}{\partial x}\left(Kh\frac{\partial u}{\partial x}\right), \quad (1)$$

$$\frac{\partial v}{\partial t}=-u\frac{\partial v}{\partial x}-\frac{E^*v}{h}+\frac{\tau_{0y}}{\rho h}-fu+\frac{1}{h}\frac{\partial}{\partial x}\left(Kh\frac{\partial v}{\partial x}\right), \quad (2)$$

$$\frac{\partial T}{\partial t}=-u\frac{\partial T}{\partial x}-\frac{E^*(T-T_0)}{h}+\frac{S}{h}+\frac{1}{h}\frac{\partial}{\partial x}\left(Kh\frac{\partial T}{\partial x}\right), \quad (3)$$

and

$$\frac{\partial h}{\partial t}=-u\frac{\partial h}{\partial x}-h\frac{\partial u}{\partial x}+E+\frac{\partial}{\partial x}\left(K\frac{\partial h}{\partial x}\right). \quad (4)$$

It has been tacitly assumed that, for the lower layer, $u_0=v_0=0$ and $h_0=\infty$. Time is represented by t while x stands for the northward-directed coordinate on a beta plane; time differencing is forward, and space differencing is upstream, as in the air model. No equatorward advection is allowed across the lateral boundaries at latitudes 30°S and 30°N. All zonal space derivatives are assumed zero. The density ρ is assumed to be 1 g/cm^3; τ_{0x} and τ_{0y} are respectively the northward and westward components of the surface wind stress, computed by the air model. The reduced gravity g' is computed by

$$g'=g\alpha(T-T_0) \quad (5)$$

where $g=980$ cm/s^2 is the standard acceleration of gravity and α, taken as 2.1×10^{-4} °K^{-1}, is the thermal expansion coefficient of water at 20°C, zero salinity and one atmosphere pressure. The Coriolis parameter f is assumed to vary linearly with x. The net downward heat flux at the sea surface S is obtained by the expression

$$S=\frac{R\downarrow-\epsilon\sigma T^4-(H_S+H_L)}{\rho c} \quad (6)$$

where $c=1$ cal · g^{-1} · °K^{-1} is the specific heat of water, $\sigma=1.355\times10^{-12}$ cal · cm^{-2} · s^{-1} · °K^{-4} is the Stefan-Boltzmann constant, and H_S and H_L are respectively the *upward* surface fluxes of sensible and latent heat as computed by the air model. The downward shortwave radiative flux $R\downarrow$ and the net longwave emissivity ϵ are obtained by

$$R\downarrow=0.94(1-0.68\,n)\,R_0 \quad (7)$$

and

$$\epsilon=0.985(0.39-0.05\sqrt{e})(1-0.6\,n^2). \quad (8)$$

Here, R_0 is the average daily clear-sky shortwave radiation flux, assumed a constant 7.95×10^{-3} cal · cm^{-2} · s^{-1} for present purposes; e is the vapor pressure of the surface air in millibars, obtained from the air model; and n is the cloudiness of the sky in tenths. Using data from the air model, we have assumed $n=0.0$ if no precipitation is occurring overhead or nearby (i.e., one grid interval away), $n=0.5$ if precipitation is occurring nearby only, and $n=1.0$ if there is precipitation overhead. Expressions (7) and (8) are taken from Kraus and Rooth (1961). Note that S has the dimensions (velocity × temperature).

Further, we have the entrainment parameter E of dimensions (velocity); this variable represents the entrainment of underlayer water into the surface mixed layer with resulting modification of this upper layer by vertical mixing; it is computed by

$$E=\frac{C_EU_*^3+C_E'(u^2+v^2)^{3/2}}{g'h}-\frac{S}{T-T_0}. \quad (9)$$

Here, U_* is the surface friction velocity computed with respect to *water* density, $C_E=5.0$ is an empirically determined constant coefficient (derived from Turner 1969) allowing some of the downward-surface turbulent kinetic-energy flux to assist the mixing process at the thermocline, and $C_E'=1.0\times10^{-5}$ is a similar coefficient representing the part of the mixing process associated with vertical current shear. This value of C_E' was chosen so that the wind-stress and current-shear contributions to mixing would be of approximately equal magnitude in equatorial latitudes. Note that the surface heat flux S is made to reduce the thermocline mixing in the sense that downward heat flux tends by itself to establish a shallower, and warmer, surface mixed layer. If S should become sufficiently large to make E negative, a re-formation of the surface layer at shallower h is indicated; in this circumstance, there is effectively no mixing of momentum or heat across the thermocline. Therefore, E is replaced by E^* in the momen-

tum and temperature equations where

$$E^*=\begin{cases} E \text{ if } E\geq 0 \\ 0 \text{ if } E<0 \end{cases}. \tag{10}$$

Lastly, K is the horizontal diffusivity; in this sea model, it has been found that the variable form discussed by Smagorinsky et al. (1965, p. 730) helps to establish a realistic latitudinal profile of surface temperature. For one horizontal dimension only, this particular diffusivity is expressed by

$$K=\frac{1}{2}(k_0\Delta x)^2\left[\left(\frac{\partial u}{\partial x}\right)^2+\left(\frac{\partial v}{\partial x}\right)^2\right]^{1/2} \tag{11}$$

where k_0 is an empirical coefficient supposed by Smagorinsky to be equal to von Kármán's constant (0.40) and Δx is the horizontal grid spacing. Note that the horizontal diffusion terms in the momentum and heat equations are conservative of the vertically integrated momentum components ρuh and ρvh and of the vertically integrated enthalpy ρcTh, redistributing them only. In constrast, the "horizontal diffusion" term

$$\frac{\partial}{\partial x}\left(K\frac{\partial h}{\partial x}\right)=\frac{1}{h}\frac{\partial}{\partial x}\left(Kh\frac{\partial h}{\partial x}\right)-\frac{K}{h}\left(\frac{\partial h}{\partial x}\right)^2 \tag{12}$$

is dissipative of the integrated potential energy ρgh^2 because of the negative-definite part in $(\partial h/\partial x)^2$; this somewhat unusual term in the continuity equation represents mass mixing by meridional plane eddies at the bottom of the surface layer in analogy to mixing by horizontal plane eddies at the edge of fast currents such as the Gulf Stream; see Stommel (1966, p. 54). Without it, uncontrolled deepening of the surface layer in regions of persistent horizontal convergence would occur in our model, as has been verified by numerical experiment.

4. RESULTS FROM THE COMBINED AIR-SEA MODEL

It has been possible to combine the air model described in section 2 with the sea model of section 3 to make a fully interacting two-fluid experiment. The 88 days of model time required about 7.5 hr of computer time on the CDC 6600 at the National Center for Atmospheric Research; horizontal grid spacing in the sea was the same as that in the air as was the forward time step—see section 2.

Some time after the completion of this experiment, two deviations from the theory of section 3 were found in the computer code. First, the pressure-gradient term $-(\partial/\partial x)(g'h)$ of eq (1) had been represented as $-g'(\partial h/\partial x)$. Subsequent comparative tests of the sea model running alone, forced by a typical surface stress profile derived from the data of Hellerman (1967), showed only very small differences in the momentum, depth, and temperature profiles of the cases with differentiated and undifferentiated g'. Second, the first coefficient of eq (11) was set equal to 2 rather than 1/2, effectively doubling

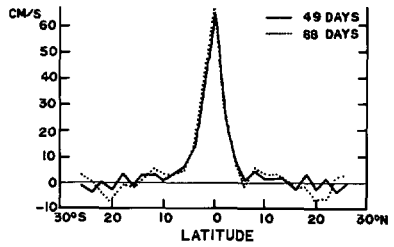

FIGURE 5.—Zonal surface ocean-current component, two-fluid case.

the value of k_0 from 0.4 to 0.8. Subsequent tests with the forced sea model showed that computed momentum, depth, and temperature profiles were much more realistic with the larger k_0; in fact, all that may accurately be said about this particular constant is that it appears to be of order unity. It appears, therefore, that the validity of our present experimental results has not been significantly reduced by the above changes.

The initial latitudinal profiles of mixed-layer depth h and underlayer temperature T_0 were given by

$$h(x)=75-25\cos\left(\pi\frac{x}{x_{30}}\right)m \tag{13}$$

and

$$T_0(x)=15+5\cos\left(\frac{\pi}{2}\frac{x}{x_{30}}\right)°\text{C} \tag{14}$$

where x_{30} is the value of the x coordinate at 30°N. Expression (13) was chosen as a very rough first-order approximation to the observed Pacific thermocline data of Wyrtki (1964); expression (14), in conjunction with the other free parameters, seemed to influence the development of a realistic surface-temperature profile, the initial form of which was identical to that in case I of section 2—see figure 1. Of course, the above depth profile was allowed to vary in time while the above underlayer temperature profile was held constant. The initial surface current was zonal and geostrophic; as its maximum magnitude did not exceed 2 cm/s, much less than what later developed, it is not shown in the following figures.

Unfortunately, a computer output tape covering the period of model time 11 through 48 days was lost during the two-fluid experiment. Because of economic considerations, the computation could not be repeated; therefore, the detailed evolution of the model parameters cannot be discussed. However, it will be shown that the major features were changing only slowly at the end of the computation. Figure 5 shows the north-south profiles of zonal surface current, positive westward, at 49 and 88 days. By far the most important feature is a sharply peaked westward equatorial current; its top value of 65 cm/s is just under 1.3 kt. It is clearly produced by the westward surface wind stress in low latitudes. The corrugated nature of this profile poleward of latitude 15° is a curious feature not readily explainable; it does not appear in any of our forced sea experiments. Not shown

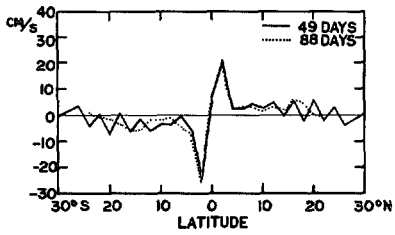

FIGURE 6.—Meridional surface ocean-current component, two-fluid case.

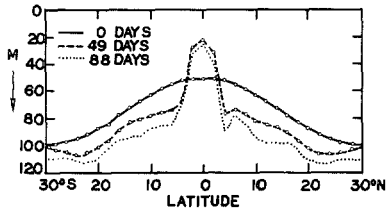

FIGURE 7.—Surface ocean mixed-layer depth, two-fluid case.

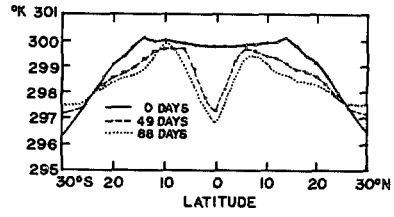

FIGURE 8.—Surface temperature, two-fluid case.

in figure 5 are two spurious westward currents that developed right at the lateral boundaries; these, too, did not appear in the forced sea model. Further research into the dynamics of two-fluid interaction is needed to explain such unexpected features; they may be influenced by the fluctuating surface wind stress produced in an interacting air-sea model in association with Coriolis effects.

The profiles of meridional surface current in figure 6 are intimately related as effect to the zonal current and to the meridional variation of Coriolis acceleration (beta effect) as cause. In both hemispheres, this acceleration is poleward, and thus divergent, on a westward current centered at the Equator; poleward current components are developed on both sides of the Equator in this case. The surface horizontal divergence has a maximum of about 1.1×10^{-6} s^{-1} right on the Equator; similar magnitudes of convergence occur at 3°S and 3°N. Unfortunately, corrugations similar to those in the zonal current are present in the meridional component as well, as are spurious poleward components at the lateral boundaries at 88 days. This latter feature, not shown in the figure, lags behind its zonal counterpart in evolution and is certainly a secondary development produced by the Coriolis acceleration. None of these curiosities appeared in the forced sea model.

Figure 7 shows the profiles of surface mixed layer depth at the initial time and at 49 and 88 days. This profile's development is obviously related to the divergence-convergence pattern implied by figure 6. Over the first 49 days, the mixed layer has become shallower in the equatorial region of horizontal divergence but deeper at higher latitudes where surface convergence is the rule. On and very near the Equator, vigorous entrainment balances the strong divergence with the maximum value of the parameter E, on the Equator, reaching as high as 3×10^{-3} cm/s; our calculations show that E is relatively small or even negative at 2° or more of latitude off the Equator. Between 49 and 88 days, there is an insidious deepening of the mixed layer at all latitudes; the active equatorial entrainment has not been completely balanced by poleward mass transport. One basic problem is that a meridional plane model cannot include explicitly the mass removal effects of a western boundary current.

Inclusion of a simple sea model in this investigation has as its major objective the prediction of surface temperature; figure 8 presents the results. When comparing this figure with the temperature profiles in section 2, it should be recalled that the units of figure 8 are actual temperature while those of the earlier figures are potential temperature; there is not much difference between the two at sea level. As expected, the vigorous entrainment on the Equator produces a marked cooling of the sea surface there; this cooling slows down markedly but does not stop completely during the later phase of the computation. The maximum surface temperature is established at an average position, over both hemispheres, of latitude 8°; and the average depression of temperature from its maximum to the equatorial value is 3°C at 88 days. In fact, the 88-day surface-temperature profile predicted by the two-fluid experiment is very similar to the fixed profile of case II of the forced air model; see figure 3. Admittedly, the interacting model does predict more equatorial cooling (an excess lowering of almost 1°C) than desired and does not behave very well at the lateral boundaries, showing unexpected warming there, probably because R_0 is held constant with latitude. Careful experimental variation of this and the other free parameters, notably k_0 in the horizontal diffusivity approximation, should improve the situation.

However, the overall performance of our simple model in surface-temperature prediction has satisfactorily revealed the expected equatorial cooling. Since the atmospheric part is sensitive to only one variable of the oceanic part (the temperature), one may expect interesting and realistic developments in the air model. Figure 9 shows the evolution of atmospheric vertical motion at 9.6 km for the two-fluid case. There is no vertical motion initially; but by 1 day, the familiar double updraft at 6°S and 6°N has developed just as in the forced air cases. This feature merges to a single equatorial updraft by 3 days; so far, the model ITCZ is behaving generally as it did in case I (sec. 2) with a flat surface-temperature profile. By 10 days,

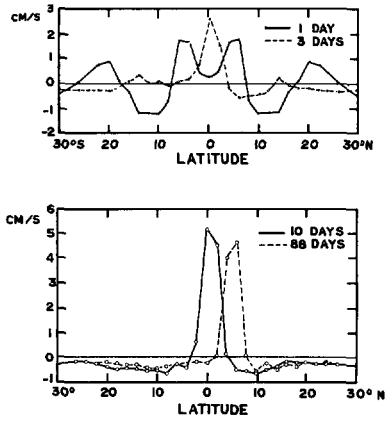

FIGURE 9.—Evolution of atmospheric vertical motion at 9.6 km, two-fluid case.

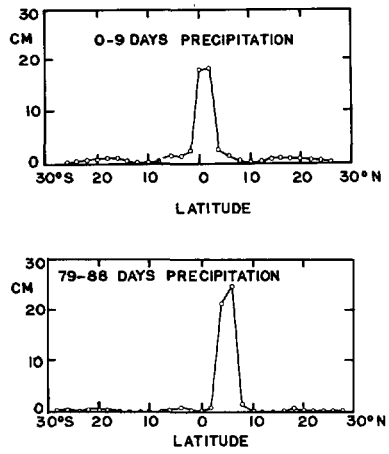

FIGURE 10.—Nine-day precipitation profiles, two-fluid case.

the ITCZ shows a tendency to start moving off the Equator; at this time, equatorial surface cooling is still negligible. Thereafter, as far as may be told from the incomplete computer output, the ITCZ moves slowly but progressively poleward; by the end of the experiment at 88 days, it has reached 6°N, directly over one of the predicted surface-temperature maxima. Obviously, the ITCZ seems to be closely attached to the local heat source, both sensible and latent, that a warm sea-surface provides.

The gross evolution of the precipitation profile for this case is seen in figure 10. Over the first 9 days of the experiment, when there is no pronounced dip in surface temperature at the Equator, the heaviest precipitation is centered no more than 2° of latitude away. Over the last 9 days, though, the heaviest rainfall is located with the maximum updraft over one of the well-defined temperature peaks at 6°N.

It is noteworthy that, as the Equator cools, the model ITCZ does not split into two parts, each one centered over a temperature maximum. Instead, the single equatorial ITCZ at 3 days maintains its identity while moving poleward, by chance toward the north, following the warm water. It appears that the great stability of this well-developed feature prevents any breakdown into a double mode over the limited time of the computation; note that, in case II of the forced air model, the intensification of one branch of a double ITCZ was accompanied by weakening of the other branch. The single ITCZ, once formed, seems to be very persistent, regardless of antecedent conditions. Truncation error in the pressure computations probably accounts for the early, small asymmetries which can grow with time. The physically meaningful results accompanying the later, large asymmetries are the single nature of the ITCZ and its location over a relatively warm surface; the particular hemisphere into which it moved is not significant in this model.

Of course, the differences between hemispheres in the real atmosphere are intimately related to three-dimensional effects accompanying the distribution of land and sea. This simple model cannot include such effects but only suggests in a general way what form the zonally averaged ITCZ is likely to take in the presence of irregular perturbations.

5. COMPARISON OF RESULTS WITH SATELLITE OBSERVATIONS

For brevity, no satellite cloud pictures will be presented here; instead, references will be given to some of the original publications containing relevant photographic or interpretive material.

A word of caution is in order when comparing results from a highly experimental fluid model with observations of the real atmosphere. Since the model is bound to be less complex than reality, its conclusions will always appear to be more straightforward than those drawn from careful and comprehensive direct observations. Probably the best compromise is to consider only those more gross observed features that have obvious counterparts, whether accurately or crudely reproduced, in the model.

It may be fairly assumed that theoretically computed precipitation maxima should be ideally associated with observed total cloudiness maxima, but not vice versa because of nonprecipitating or low-precipitating stratiform clouds. Since our two-fluid model suggests that the equilibrium position of the oceanic ITCZ rainfall peak is a few degrees of latitude away from the Equator, it is encouraging to note that Sadler (1969), using carefully analyzed satellite data for 1965 and 1966, finds that the latitude of maximum cloudiness in the Tropics, averaged over all longitudes and taking an average of winter and summer, is 5°N; see his figure 4. Sadler does not present a sea-surface temperature analysis for the same period as that of his observations, nor does any other published satellite cloudiness study; thus, no direct substantiation of our theoretical findings with respect to the surface temperature pattern is to be had from satellite pictures.

One may only assume that long-term climatological temperature maps such as those by Defant (1961) are characteristic of much shorter periods, if only in very low latitudes.

Kornfield and Hasler (1969) present data comparable to Sadler's, but for the year 1967 and in the form of computer produced time-averaged pictures rather than processed diagrams. The oceanic ITCZ in these photographs clearly stays several degrees of latitude away from the Equator all year in the Pacific and most of the year, except for the late northern winter and early spring, in the Atlantic. In the Indian Ocean, strong monsoonal influences complicate the situation; but it is suggested from both these and Sadler's data that here the Equator is more hospitable to occasional ITCZ formation than over other seas. Fortunately, Defant's maps do indicate that equatorial cooling is far less pronounced over the Indian Ocean all year and over the Atlantic during the northern winter than it usually is over the eastern and central Pacific. An off-Equator ITCZ is certainly observed over the western Pacific where the equatorial surface does not show nearly as pronounced a temperature drop in meridional profile as it does farther east; but this feature may be strongly influenced by zonal advection of heat and moisture, from the east, that our two-dimensional model cannot duplicate in its meridional plane.

An interesting note by Hubert et al. (1969), using a year of satellite data partially overlapping those of Kornfield and Hasler, concludes that a single pronounced ITCZ cloudiness maximum with respect to latitude is much more common than a pronounced double maximum (i.e., that the actual ITCZ is usually hemispherically very asymmetric when off the Equator). This observation applies at sea as well as over land and is implicitly confirmed by the two other sources just discussed; it is tempting to establish some connection between it and our experimental results that a double ITCZ can have an unstable character in that one of its branches can dominate the other as in section 2 (case II) while a single ITCZ appears to be comparatively stable, on or off the Equator, as in section 2 (case I) and in section 4. For the moment, all that may be said is that these observations do not conflict with our notion that the single ITCZ is the more stable configuration.

6. SUMMARY

Several experiments with a primitive-equation model of the tropical atmospheric circulation in a meridional plane indicate clearly that the location and structure of the oceanic ITCZ are influenced by the north-south profile of sea-surface temperature. A definite maximum in surface temperature, on or off the Equator, encourages atmospheric convergence, upward motion, and active precipitation overhead or nearby. In the case of a relatively flat profile, the major convergence zone forms over the Equator, just as if there had been a temperature maximum there; in our model, an equatorial temperature depression seems necessary to keep the ITCZ away. Here is good motivation to develop an interacting two-fluid model, including the upper ocean, to predict the surface-temperature profile and its effects on tropical convection. Results from such a model, with an initially flat profile, show the progressive development of a cold Equator as a result of upwelling and vertical mixing of cold water in the sea. A single ITCZ establishes itself at first over the Equator but then migrates poleward as the Equator cools; the convergence zone remains single, despite the eventual double surface-temperature maximum. This marked hemispheric asymmetry appears to be of the same type one notices very often in satellite cloud pictures of the oceanic ITCZ.

A numerical integration of the two-fluid model over a period of several years is desirable to investigate the degree of stability of the single off-equatorial ITCZ under the influence of seasonally variable solar heating of the sea. Of course, hemispheric asymmetries in the real atmosphere and ocean must be influenced primarily by the geographical differences in land and sea distribution between the hemispheres; a meridional plane model such as ours cannot take these factors into account. However, the mere production of experimental asymmetries by this model suggests that the real ones it mimics may be at least partially generated internally rather than entirely forced by events at higher latitudes.

Even with the present relatively simple interacting model, almost 8 hr of fast computer time is required for a 3-mo prediction. To compute just one experiment over 3 yr of model time would then require machine time approaching 100 hr, an unacceptable amount to anyone without unlimited access. Simplification of the model is indicated: since the oceanic part is about as basic as can be safely attempted in temperature prediction involving dynamic factors, only the atmospheric part could safely be reduced in complexity. Some decrease in vertical resolution would probably be the least harmful procedure; a three layer primitive-equation air model such as that of Yamasaki (1968) is an attractive possibility.

ACKNOWLEDGMENTS

This research was mainly sponsored under Contract No. F19628-68-C-0144 with the U.S. Air Force Cambridge Research Laboratories.

Many thanks are due Prof. Mariano Estoque and Dr. Stanley Rosenthal for helpful and encouraging advice with respect to the atmospheric part of this work and to Profs. Eric Kraus and Claes Rooth with respect to the oceanic part. The author is grateful to Dr. Michael Hantel for many consultations during the development and testing of the two-fluid model. Preparatory work on the programming of the model for electronic computation was done on the IBM 7040 and 360/65 computers at the University of Miami; production runs were made on the CDC 6600 at the National Center for Atmospheric Research, sponsored by the National Science Foundation. The manuscript of this paper was typed by Miss Janet Sargent, and the figures were prepared by Mr. Richard Dirks and Mrs. Lynn Gheer.

REFERENCES

Defant, Albert, *Physical Oceanography*, Vol. 1, Pergamon Press, New York, N.Y., **1961**, 729 pp.

Estoque, Mariano A., "Vertical Mixing Due to Penetrative Convection," *Journal of the Atmospheric Sciences*, Vol. 25, No. 6, Nov. **1968**, pp. 1046–1051.

Estoque, M. A., and Bhumralkar, C. M., "Flow Over a Localized Heat Source," *Monthly Weather Review*, Vol. 97, No. 12, Dec. **1969**, pp. 850–859.

Hellerman, S., "An Updated Estimate of the Wind Stress on the World Ocean," *Monthly Weather Review*, Vol. 95, No. 9, Sept. **1967**, pp. 607–626 (also see corrected tables in Vol. 96, No. 1, Jan. 1968, pp. 63–74).

Hubert, L. F., Krueger, A. F., and Winston, J. S., "The Double Intertropical Convergence Zone: Fact or Fiction?," *Journal of the Atmospheric Sciences*, Vol. 26, No. 4, July **1969**, pp. 771–773.

Kornfield, Jack, and Hasler, A. Frederick, "A Photographic Summary of the Earth's Cloud Cover for the Year 1967," *Journal of Applied Meteorology*, Vol. 8, No. 4, Aug. **1969**, pp. 687–700.

Kraus, Eric B., and Rooth, Claes, "Temperature and Steady State Vertical Heat Flux in the Ocean Surface Layers," *Tellus*, Vol. 13, No. 2, Stockholm, Sweden, May **1961**, pp. 231–238.

Kraus, Eric B., and Turner, J. Stewart, "A One-Dimensional Model of the Seasonal Thermocline: Part II. The General Theory and Its Consequences," *Tellus*, Vol. 19, No. 1, Stockholm, Sweden, **1967**, pp. 98–106.

Murgatroyd, R. J., "Estimations From Geostrophic Trajectories of Horizontal Diffusivity in the Mid-Latitude Troposphere and Lower Stratosphere," *Quarterly Journal of the Royal Meteorological Society*, Vol. 95, No. 403, London, England, Jan. **1969**, pp. 40–62.

Peixoto, José Pinto, "Hemispheric Temperature Conditions During the Year 1950," *Planetary Circulations Project, Scientific Report* No. 4, Contract No. AF19(604)–6108, Department of Meteorology, Massachusetts Institute of Technology, Cambridge, **1960**, 211 pp.

Peixoto, José Pinto, and Crisi, A. R., "Hemispheric Humidity Conditions During the IGY," *Planetary Circulations Project, Scientific Report* No. 6, Contract No. AF19(628)–2408, Department of Meteorology, Massachusetts Institute of Technology, Cambridge, **1965**, 166 pp.

Pike, Arthur C., "A Numerical Study of Tropical Atmospheric Circulations," *Scientific Report* No. 1, Contract No. AFCRL–68–0593, Air Force Cambridge Research Laboratories, Bedford, Mass., **1968**, 129 pp.

Richtmyer, Robert D., and Morton, K. W., *Difference Methods for Initial-Value Problems*, 2d Edition, Interscience Publishers, New York, N.Y., **1967**, 405 pp.

Rosenthal, Stanley L., "A Circularly Symmetric Primitive Equation Model of Tropical Cyclone Development Containing an Explicit Water Vapor Cycle," *Monthly Weather Review*, Vol. 98, No. 9, Sept. **1970**, pp. 643–663.

Sadler, James C., *Average Cloudiness in the Tropics From Satellite Observations*, East-West Center Press, Honolulu, Hawaii, **1969**, 23 pp.

Smagorinsky, Joseph, Manabe, Syukuro, and Holloway, J. Leith, Jr., "Numerical Results From a Nine-Level General Circulation Model of the Atmosphere," *Monthly Weather Review*, Vol. 93, No. 12, Dec. **1965**, pp. 727–768.

Stommel, Henry, *The Gulf Stream*, University of California Press, Berkeley, **1966**, 248 pp.

Turner, J. Stewart, "A Note on Wind Mixing at the Seasonal Thermocline," *Deep-Sea Research*, Vol. 16, Supplement, Oxford, England, Aug. **1969**, pp. 297–300.

U.S. Weather Bureau, *World Weather Records, 1941–50*, Washington, D.C., **1959**, 1361 pp.

Wyrtki, Klaus, "The Thermal Structure of the Eastern Pacific Ocean," *Deutsche Hydrographische Zeitschrift, Ergänzungsheft*, Ser. A, No. 6, Hamburg, Germany, **1964**, 84 pp.

Yamasaki, Masanori, "A Tropical Cyclone Model With Parameterized Vertical Partition of Released Latent Heat," *Journal of the Meteorological Society of Japan*, Vol. 46, No. 3, Tokyo, June **1968**, pp. 202–214.

[*Received May 27, 1970; revised January 7, 1971*]

CORRECTION NOTICE

Vol. 99, No. 2, Feb. 1971: p. 149, left col., eq, r is to be read instead of 2; p. 153, left col., line 14, 11 is to be read instead of 4.